

NJC

Accepted Manuscript



This article can be cited before page numbers have been issued, to do this please use: Y. Li, G. Li, J. Li and Y. Luo, *New J. Chem.*, 2018, DOI: 10.1039/C7NJ03841K.



This is an Accepted Manuscript, which has been through the Royal Society of Chemistry peer review process and has been accepted for publication.

Accepted Manuscripts are published online shortly after acceptance, before technical editing, formatting and proof reading. Using this free service, authors can make their results available to the community, in citable form, before we publish the edited article. We will replace this Accepted Manuscript with the edited and formatted Advance Article as soon as it is available.

You can find more information about Accepted Manuscripts in the [author guidelines](#).

Please note that technical editing may introduce minor changes to the text and/or graphics, which may alter content. The journal's standard [Terms & Conditions](#) and the ethical guidelines, outlined in our [author and reviewer resource centre](#), still apply. In no event shall the Royal Society of Chemistry be held responsible for any errors or omissions in this Accepted Manuscript or any consequences arising from the use of any information it contains.



NJC

PAPER

Preparation and properties of semi-interpenetrating networks combined by thermoplastic polyurethane and thermosetting elastomer

Yajin Li,^a Guoping Li^a, Jie Li and Yunjun Luo^{*a}Received 00th January 20xx,
Accepted 00th January 20xx

DOI: 10.1039/x0xx00000x

www.rsc.org/

Thermosetting elastomer has been introduced into hydroxyl-terminated polyether thermoplastic polyurethane systems by semi-interpenetrating technology. The novel energetic macromolecule materials are investigated by Fourier transform infrared spectroscopy (FTIR), uniaxial tensile test, dynamic mechanical analysis (DMA) and thermal gravimetric analysis (TGA), respectively. The results show that this material has good mechanical properties with stress of 9.7 MPa and strain of 1010.7 % when the mass percentage of triazole segments is 20 wt. %. It is worth noticing that the network structure parameters of semi-interpenetrating materials are quantitatively calculated for the first time based on the relationship between elastic modulus and effective crosslinking density. The damping analysis results present that the linear polyurethane domains are tightly embedded into the tridimensional network of triazole domains. In addition, it is confirmed from thermal stability and energy analysis that the samples exhibit good thermal stability and positive heat of formation. Therefore, the novel energetic materials are of potential applied value in the area of aerospace industry and missile technology.

Introduction

The polymeric binders in propellants are normally cross-linked polyurethane networks, which function as a matrix to combine some additives (such as oxidizers and metal fuels).¹⁻³ Hydroxyl-terminated polyether type thermoplastic elastomers (HTPEs) as the linear polymer have been widely used as polymeric binders for the preparation of nitrate ester polyether (or polyester) (NEPE) propellants due to the excellent low-temperature mechanical properties since this century.⁴⁻⁶ In these HTPEs, poly(ethylene oxide-co-tetrahydrofuran) (PET) polymer is composed of ethylene oxide (EO) and tetrahydrofuran (THF), in which the THF segments offer a superior strength and low-temperature property while the EO segments give rise to a favorable flexibility.⁷ Although the PET-based propellants have a wide range of mechanical properties, PET polymeric binder does not possess rich enthalpy which greatly limited the energy level of propellants. Therefore, to develop a high performance polymeric binder is the goal for researchers, and many attempts have been made to improve this situation via blending polyether polymer with energetic binders which have positive heat of formation, for example, glycidyl azide polymer (GAP) binder.

GAP is considered to be a promising binder for propellant industry. It outperforms other energetic binders that have been developed in recent years due to its positive effect on the burning rate and specific impulse of propellant.⁸⁻¹⁰ Furthermore, the presence of azide groups (-N₃) in the GAP polymer chain allows it to react with end-alkynyl compounds to form triazole cross-linking networks.¹¹⁻¹³ The obtained novel cross-linked networks could not only enhance the thermal stability and burn rate in the polymeric binders,¹⁴⁻¹⁶ but form three-dimensional networks without any lateral reactions due to the moieties insensitive nature. Unfortunately, because of the rigidity for triazoles as crosslinks and the wasted loops formed by the intermolecular crosslinking, their mechanical properties are unsatisfactory. Therefore, researchers have attempted to make some improvements. For example, Min *et al.*¹⁴ have prepared a dual curing system by urethane- and triazole-forming reactions. The dual curing systems could improve the mechanical properties than the single triazole network, and the new system based solid propellants exhibited a higher burn rate and a low pressure exponent. However, the dual system showed two low glass transition temperatures due to the incompatibility of their polymeric chains. This phenomenon limits the mechanical property improvement.

Usually, the chemical and physical combinations of two or more structurally dissimilar polymers provide a convenient route for the modification of properties to meet specific needs.¹⁷ Normal blending or mixing of two polymers result in a multiphase morphology due to thermodynamic incompatibility which arise from the relatively small gain in entropy of

^a School of Materials Science & Engineering, Beijing Institute of Technology, Beijing 100081, PR China. E-mail: yjluo@bit.edu.cn; Fax: +86 010 68913698; Tel: +86 010 68913698

Electronic Supplementary Information (ESI) available: [details of any supplementary information available should be included here]. See DOI: 10.1039/x0xx00000x

mixing.¹⁸ If mixing takes place on a lower molecular weight level and polymerization is carried out simultaneously with crosslinking, phase separation may be kinetically controlled as the entanglements are made permanent by crosslinking. Interpenetrating polymerization represents a third mechanism by which different polymers can be physically combined.^{19,20} In general case, a network in which one or more polymers are cross-linked, one or more polymers are linear or branched is named as semi-interpenetrating elastomer networks (semi-IENs). Considering the advantages of HTPEs and triazole network, we construct a novel triazole-polyurethane latex semi-IENs.

In this study, a series of semi-interpenetrating elastomer networks of PET-TPEs with triazole polymer have been obtained by the sequential-IPN process. The prepared semi-IENs were investigated with Fourier transform infrared spectroscopy (FTIR), uniaxial tensile test, dynamic mechanical analysis (DMA) and thermal gravimetric analysis (TGA), respectively. It is expected to provide a novel binder system for the area of aerospace industry and missile technology.

Experimental

Materials

Poly (Ethylene Oxide-co-Tetrahydrofuran) (PET, analytical grade, $M_n = 4000$ g/mol) was obtained from Hubei Aviation Institute of Chemical Technology and purified by vacuum drying. Isophorone diisocyanate (IPDI, Bayer (Germany); $M_n = 222.29$ g/mol) was used as received. 1,4-Butanediol (BDO, analytical grade, $M_n = 90$ g/mol) was obtained from Beijing Chemical Plant and used after it was vacuum-dried for 4h at 85 °C. The catalyst was prepared by the dissolution of dibutyl tin dilaurate (Beijing chemical plant) into diethyl phthalate.

Glycidyl azide polymer (GAP, $M_n = 3600$ g/mol) was obtained from Liming Research Institute of Chemical Industry and purified by vacuum drying for 2h at 80 °C. Acyl-GAP was synthesized by our teams work in recent report²¹ (synthesis route see Scheme2). The aliphatic alkynes (BPS) was synthesized based on literature procedures²² (synthesis route in Supplementary materials Scheme 1S).

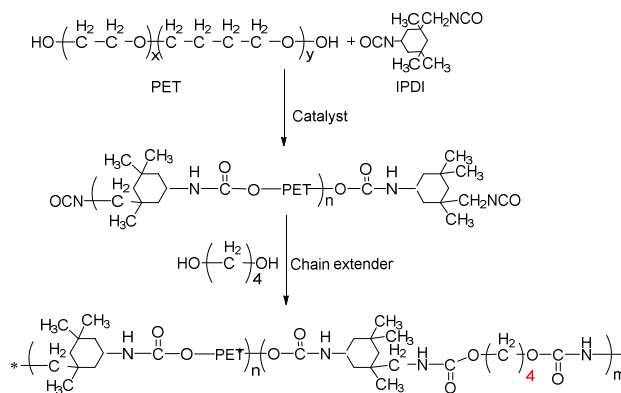
Synthesis of PET-TPEs

The PET-TPE (linear polymer) was synthesized using chain extender BDO with hard segment weight percentage ratios (HS=40 wt. %), the synthesis process was illustrated in Scheme 1. The hard segments consisted of IPDI chain-extended with BDO, while the soft segment was PET. The hard-segment content (HS) by weight was determined according to the industry's standard (the molar ratio of [NCO]/[OH] was 1.0 for all PET-TPEs samples):

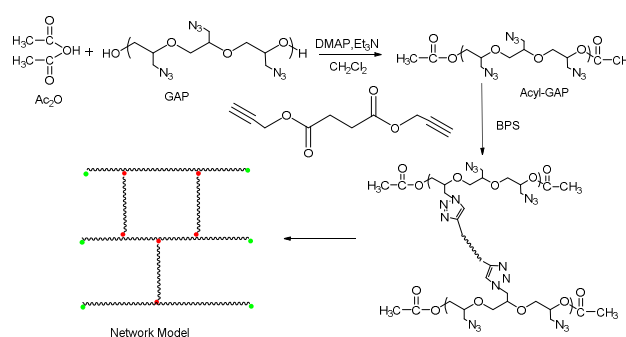
$$HS(\text{wt. \%}) = \frac{m_{IPDI} + m_{BDO}}{m_{IPDI} + m_{BDO} + m_{PET}}$$

Where m_i is the mass.

A stoichiometric amount of PET polymer was heated and stirred at 90 °C, then, the catalyst and IPDI were added. The reaction mixture was stirred and kept for 2 h at 90 °C.



Scheme 1 Synthesis route of PET-TPE. The react agent is IPDI, and the chain extender is BDO.



Scheme 2 Synthesis route of triazole system. GAP polymer reacted with acetic anhydride as end-capping; it can be sure that the system have not any lateral reactions.

BDO was added to the previous NCO-terminated PET prepolymer at 60 °C, and the reaction was kept for 20 min. Then, the product was cast in a mould to cure at 60 °C for around 96h in the nitrogen atmosphere. In the meantime, real-time monitoring of the product molecular weight was conducted by GPC testing.

Preparation of semi-IENs

The semi-IENs were prepared by *in situ* polymerization method. Scheme 2 and Fig. 1 illustrate the forming process and schematic diagram for the triazole based thermosetting system and semi-IENs, respectively. After the PET-TPE reaching a certain molecular weight, predetermined masses of the Acyl-GAP with BPS were added into the PET-TPE, and the mixture was quickly stirred around 30 min for homogenization. The mixture was poured into the Teflon mold to cure at 60 °C for around 96 h in the nitrogen atmosphere to obtain the sample. The samples with triazole system were marked as 10%-semi-IEN (10% Acyl-GAP/BPS), 20%-semi-IEN (20% Acyl-GAP/BPS), 30%-semi-IENs (30% Acyl-GAP/BPS), 40%-semi-IEN (40% Acyl-GAP/BPS) and 50%-semi-IEN (50% Acyl-GAP/BPS), respectively.

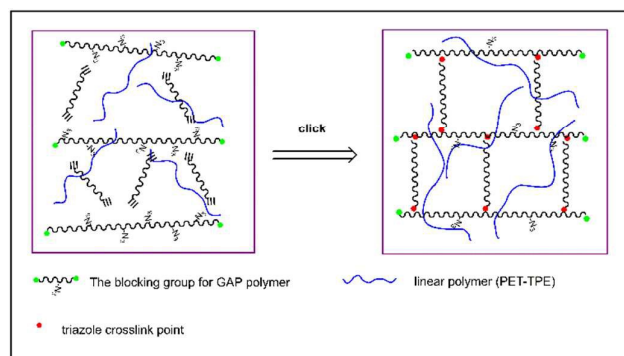


Fig. 1 Schematic route for the preparation of semi-IENs.

Measurements

Fourier transform infrared spectroscopy (FTIR) measurements were recorded (Nicolet FTIR-8700, Thermo) in the range of 4000~500 cm^{-1} .

The molecular weights were obtained using GPC (LC-20A, Shimadzu) at 35 °C using THF as the mobile phase and the flow rate was 1 ml/min. The raw data were calibrated using a universal calibration with polystyrene standards.

The mechanical properties, including the largest tensile strength (σ_m) and elongation at break (ϵ_b), of all the dumbbell-shape specimens were measured using a universal testing machine (Instron-6022, Shimadzu Co., Ltd.) at a constant rate of 100 mm/min and the results were averaged from five samples.

Dynamic mechanical analysis (DMA) was performed using METTLER Instrument DMA/SDTA861e at shear model device and a frequency of 1Hz. The temperature range was from -100 to 100 °C under a nitrogen atmosphere with a heating rate of 3 °C/min. The dimensions of the test specimens were square samples with the length 4 mm and thickness 2 mm.

The thermal gravimetric analysis (TGA) was performed on the METTLER Instrument TGA-STAR system at heating rates of 10 °C/min from 30 to 600 °C. The samples of 5 mg were used, and the flow rate of nitrogen gas was 40 ml/min.

The samples were fractured with liquid nitrogen and the microphotographs were taken after gold sputtering. Atomic force microscopy (AFM) measurement of the surface morphology of samples was conducted in air under ambient conditions using Bruker Dimension Edge.

Results and discussion

Molecular weight analysis

The number-average molecular weight (\overline{M}_n) and polydispersity index (PDI; $\overline{M}_w/\overline{M}_n$) of PET pre-polymers are listed in Table 1. The \overline{M}_n of samples gradually increases with the extension of pre-polymerization time. The PDI of the prepared PET pre-polymers is between 1.41 and 2.09, which shows that the products have high molecular weight and narrow molecular weight distribution. The formation of macromolecular polymer inevitably leads to the increase viscosity and may lead to partial crosslinking. It could be found that some gelation appeared at longer polymerization time. In Table 1, the molecular weight has a downward trend and the PDI increases when the pre-polymerization time is more than 4.5 h. In the GPC testing process, the samples (PET-5h, PET-6h) couldn't be completely dissolved, which indicates that slightly cross-linked phenomenon occurs. This phenomenon is adverse for the preparation of semi-IENs. Therefore, we selected 4.5 h as the pre-polymerization time of PET-TPEs for better preparation process in this study.

Structure characterization of semi-IENs

FTIR analysis

The prepared PET-TPE and semi-IENs were characterized to investigate their chemical structures. The FTIR spectrum of PET, IPDI, BDO and PET-TPE are shown in Fig. 2. From the FTIR spectra of pristine PET shown in Fig. 2(a), obvious characteristic peak at 3433 cm^{-1} is ascribed to the stretching vibration of O-H group and the C-O-C symmetric stretching vibration appears at 1130 cm^{-1} . The clear peaks at 2935 cm^{-1} , 2966 cm^{-1} , 2943 cm^{-1} are corresponding to the C-H vibration for the polymers. As seen from Fig. 2(b), the characteristic absorption peak at 2250 cm^{-1} belongs to the NCO stretching vibration of IPDI. In the spectra of the prepared PET-TPE, the peaks for O-H group and NCO group disappear, and a new peak of 1705 cm^{-1} is observed, which belongs to the amide carbonyl stretching vibration. The FTIR spectra of the prepared semi-IENs is shown in Fig. 3(d), and the same peak as PET-TPE (see Fig. 3(c)) still appear while the alkynyl group at 3293 cm^{-1} disappears, which indicates that the Acyl-GAP reacts with BPS but doesn't react with PET-TPE.

Table 1 The GPC results of PET pre-polymers. (The molar ratio of [NCO]/[OH] was 1.0 for all PET-TPEs samples)

Samples	PET-3h	PET-3.5h	PET-4h	PET-4.5h	PET-5h	PET-5.5h	PET-6h
\overline{M}_n (g/mol)	20426	28941	35450	38779	36532	35891	33387
PDI ^a	2.02	2.01	1.41	1.87	2.09	2.12	2.11

^a PDI: polydispersity index, calculated from $\overline{M}_w/\overline{M}_n$, where measured in GPC testing.

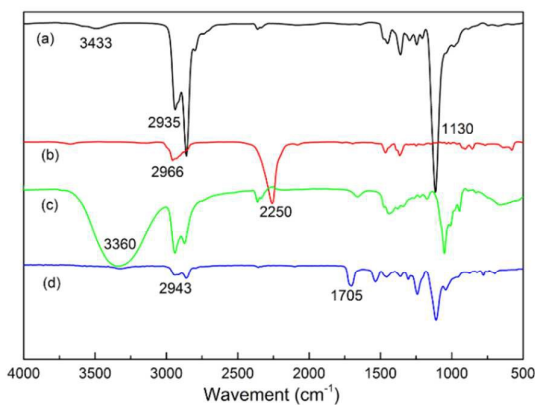


Fig. 2 FTIR spectrum of (a) PET; (b) IPDI; (c) BDO; (d) prepared PET-TPE.

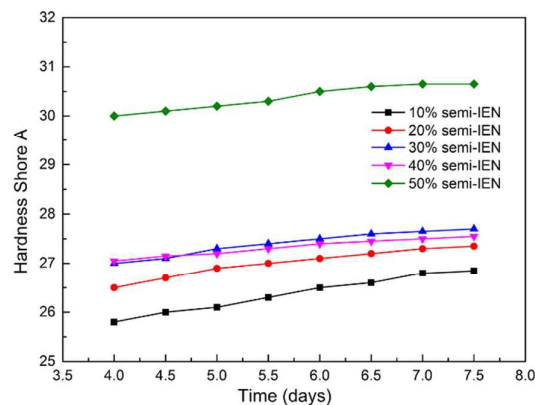


Fig. 4 Hardness testing of semi-IENs.

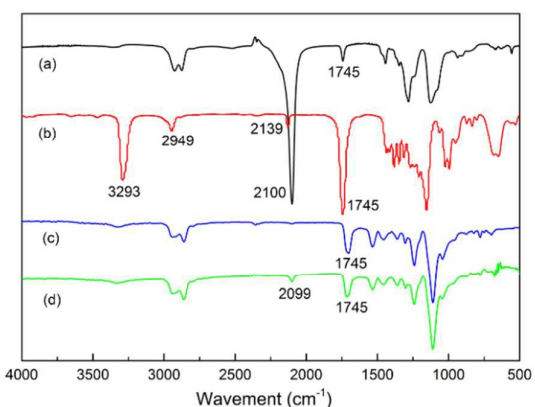


Fig. 3 FTIR spectrum of (a) Acyl-GAP; (b) BPS; (c) PET-TPE; (d) prepared semi-IENs.

Hardness analysis

The hardness of the semi-IENs samples was also measured by shore A tester according to ASTM D2240. Post curing hardness of semi-IENs system was investigated by measuring surface hardness-A till reaching a constant value.

Variations in the shore hardness-A depending upon the amount of triazole system are shown in Fig. 4. The hardness increases as the curing reaction proceeds and reaches a plateau of constant value, indicating reaction is completed. It can also be seen from Fig. 4 that the final hardness value rises with the increase of the amount of rigid crosslink points.

Micro-phase Morphology

To confirm the micro-phase morphology of the prepared semi-IEN composites, the SEM and AFM was conducted. Fig. 5 shows the SEM and AFM images of fractured surface of semi-IEN with 50 wt. % triazole system, respectively. The fractured surfaces of semi-IEN depicts smooth microstructures due to the rigid triazole crosslinks. There are large flat regions existed in the fish scale fractures, implying an enhanced mechanical properties with the formation of texture structures.

AFM provides a method to confirm the micro-phase separated nature of semi-IEN. Fig. 5(b) depicts the aggregation of rigid domains as bright regions whereas the soft matrix as the darker features.²³ The bright regions scatter around the darker regions imply a weakened micro-phase separated feature with the synergistic effect of two segments.

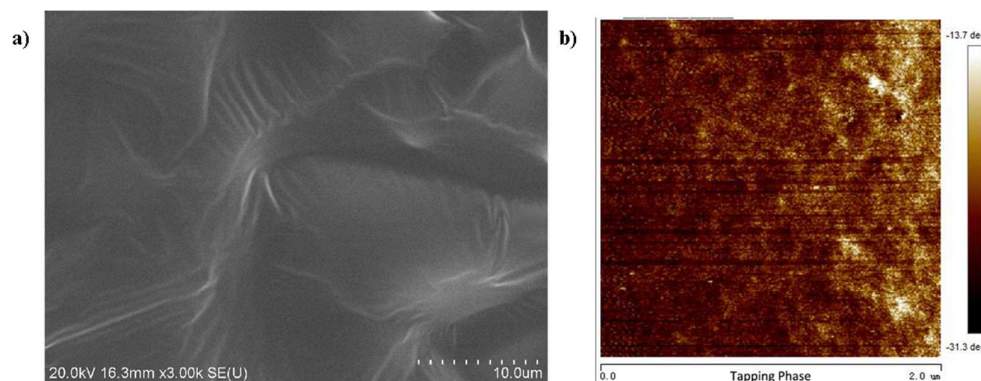


Fig. 5 (a) SEM image for the fractured surfaces of the semi-IEN. (b) AFM phase image for the semi-IEN film.

NJC

PAPER

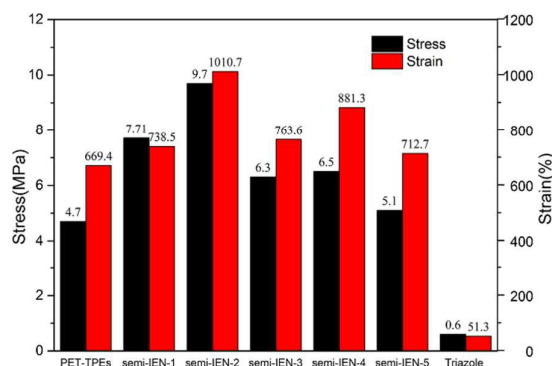


Fig. 6 Comparison of tensile stress and strain of polyurethane, triazole system and semi-IENs.

Mechanical properties

The interpenetrated and entangled chains of two polymers network can increase the phase stabilities and enhance the mechanical properties of the final products. Considering the stress and strain, we selected the PET-TPE as supporting materials in semi-IENs. As the PET-TPE can well support the mechanical, meanwhile the triazole system can increase the energy for the semi-IENs.

The tensile stress, strain of samples are illustrated in Fig. 6, as functions of triazole content. It depicts the comparison of tensile stress and strain of semi-IENs with polyurethane and triazole system. The results indicate that the semi-IENs exhibit excellent improved mechanical properties (especially stress) compared with unitary polyurethane system. When the mass percentage of triazole system is 20 wt. %, the prepared semi-IENs keep the maximal mechanical strength and elongation. The fact that the prepared semi-IENs show better mechanical properties could be based on the explanation of morphologies for fractured surfaces as described earlier.

Network structure analysis

For semi-interpenetrating elastomer networks, researchers still have little knowledge about the network structure. In the present work, we tried to quantitative the results by the effective crosslinking density (V_e). The PET-TPE sample is amorphous material and the physical crosslinking would play a key role on the mechanical properties if its chemical structure is similar. Hydrogen bond is the most important physical crosslinking effect of polyurethane (Hydrogen-bonded diagram as Fig. 7).²⁴⁻²⁶

Weisfeld et al.²⁶ have proposed that the physical crosslinking density of PU accords with the Arrhenius

relationship (Eq. (1)). For an elastomer, the elastic modulus could be expressed as the effective sum of both chemical and physical crosslinking effects (Eq. (2)). For the polyether type PUE, the chemical crosslinking effect could be negligible.²⁶ Thus, the elastic modulus with temperature could be transformed to Eq. (3).

$$V_p = A * e^{(E_a/RT)} \quad \text{Eq. (1)}$$

$$E' = V_e * RT = (V_c + V_p) * RT \quad \text{Eq. (2)}$$

$$E' = V_p * RT \quad \text{Eq. (3)}$$

Where E_a is the activation energy of physical crosslinking, E' is the elastic modulus, V_e is the effective crosslinking density, V_c is the chemical crosslinking density, V_p is the physical crosslinking density, R is the general gas constant, A is a constant, and T is the absolute temperature.

In this work, the activation energy of hydrogen bond dissociation (E_a) and the hydrogen bond density (V_p) of PET-TPE were evaluated from the elastic modulus-temperature relationship. Fig. 8 presents the elastic modulus (E') as a function of temperature between 273 and 373 K of the PET-TPE and triazole system. The values of E' decrease sharply as the temperatures increase from 273 to 373 K for PET-TPE system, and the values of E' almost remain the same level at higher temperature. This phenomenon is attributed to the hydrogen bond dissociation. Fig. 9(a) gives the relationship between V_e and temperature of PET-TPE, and the results indicate that the V_e gradually decrease with the increase of temperature for physical crosslinking density decreased. As mentioned previously, the relationship of $\ln(E'/T)$ versus $1/T$ is illustrated in Fig. 10. Table 2 shows the values of E_a , A and V_p of PET-TPE sample calculated from Fig. 10.

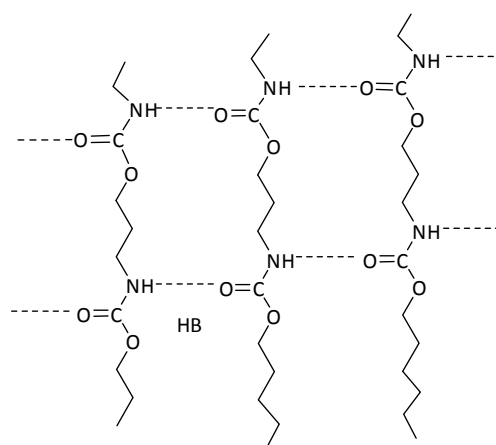


Fig. 7 Schematic representation of "chain" of hydrogen-bonded.

The hard segments of molecular are connected with each other by intermolecular hydrogen bond and form domains to act as junctions of physical crosslinking for the soft segments.^{25, 27} Fig. 8(b) shows that when temperature increases, the elastic modulus of triazole system increase due to the aggravation of thermal vibrations for polymer segments which attributed entropic contribution of the network.²⁸ For the triazole crosslinking system, there is no hydrogen bonding interaction, which means that physical crosslinking density is mainly from the chain entanglement, so the V_e has a small variation from 3.68×10^4 to 3.45×10^4 mol/cm³ with the increase of temperature (Fig. 9(b)).

To further confirm the effect of triazole polymers on network structure parameters of semi-IENs chains, the V_c and V_p are calculated based on the above theory. Using the same testing method as sample PET-TPE, semi-IENs samples were also measured by DMA at temperature between 273 and 373 K. This temperature range is above the glass transition temperature (T_g) of all samples.

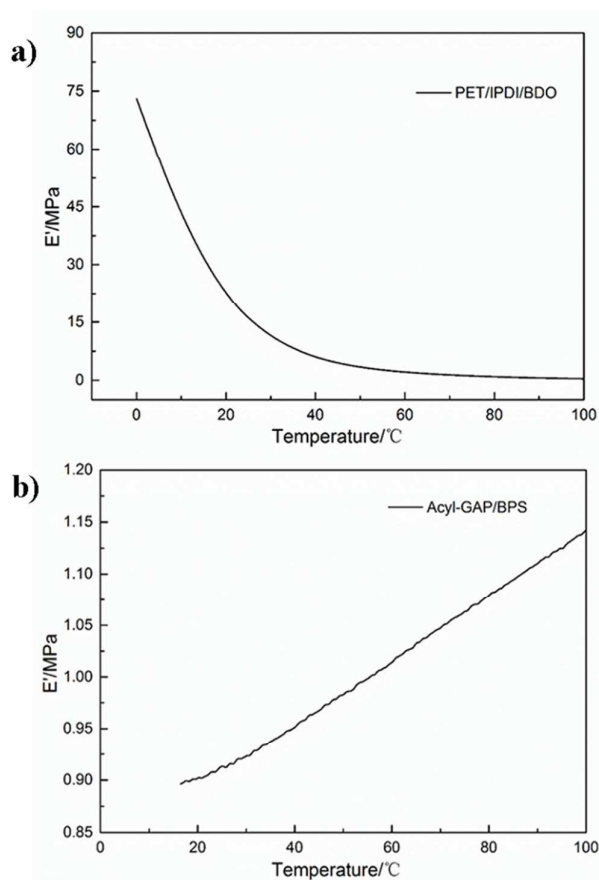


Fig. 8 Elastic modulus of polyurethane and triazole system as a function of temperature. (a) Relationship between E' and T ; (b) Relationship between E' and T .

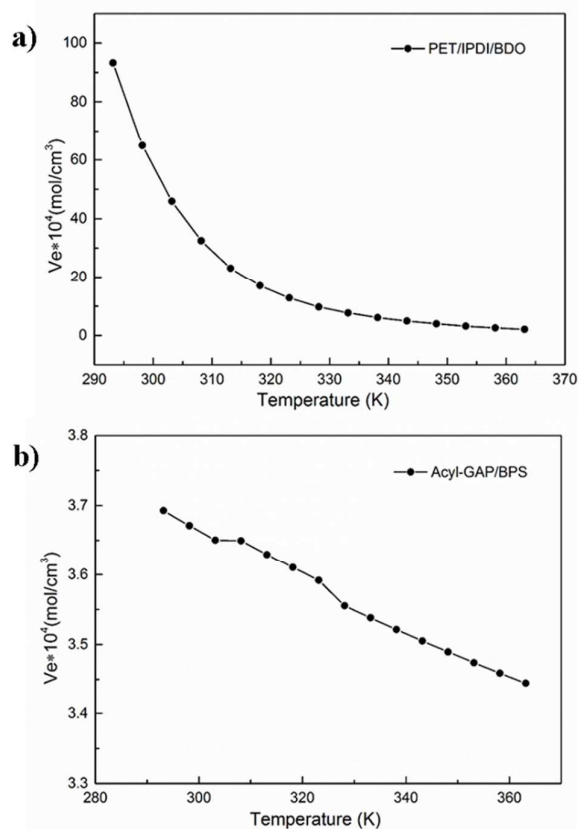


Fig. 9 Relationship between V_e and T of polyurethane and triazole system. (a) Relationship between V_e and T ; (b) Relationship between V_e and T .

Fig. 11 and Fig. 12 (a) give the variation trend of the elastic modulus and V_e of the samples, 10% to 50% semi-IENs, respectively. In the semi-IENs system, the decrease of elastic modulus indicates that the elastic modulus in this study depends strongly upon temperature.

The decrease of V_e is contributed to the decrease of physical crosslinking rather than the chemical crosslinking.²⁹ According to the previous analysis, the decrease of effective crosslinking density (V_e) between any temperatures points belongs to the extent of hydrogen bond in physical crosslinking diminishes, which can be expressed by following Eq. (4).

$$(V_e)_{T_i} - (V_e)_{T_j} = (V_p)_{T_i} - (V_p)_{T_j} = A * [e^{E_a/RT_i} - e^{E_a/RT_j}] \quad \text{Eq. (4)}$$

The values of E_a , A and V_p of samples (Acyl-GAP content is 10, 20, 30, 40, and 50 wt. % of semi-IENs) can be calculated through curve fitting as shown in Fig. 12(b) and Table 2. Fig. 13 shows the V_p and V_c as a function of temperatures, and the values of V_p have same trend with V_e but the V_c basically remain the same level.

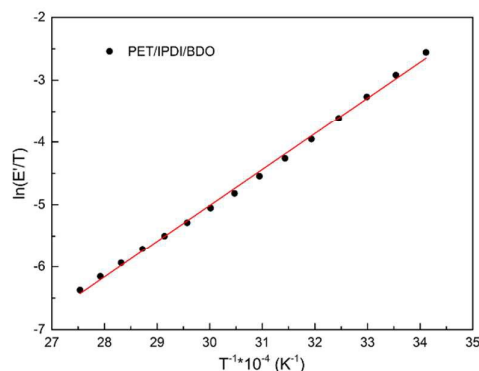


Fig. 10 Relationship between $\ln(E'/T)$ and $1/T$ of polyurethane system. Lines are the regression results.

Obviously, the quantitative data of V_p decrease with the content of triazole system increase at 25 °C, while the V_c have no significant change indicating that more topological entanglement between molecular chain arise. When temperature increases, the hydrogen bond effect diminishes and the V_p of elastomers almost overlap. For semi-IENs samples, they have similar chemical structures but the interpenetrating percentages are different. The physical crosslinking contribution to the elastic modulus decrease with the temperature increase (see Fig. 14), which indicates that physical crosslinking plays an indispensable role on the tensile properties especially at ambient temperature.

Damping properties

The $\tan \delta$ responses of semi-IENs samples measured by DMA are shown in Fig. 15. Fig. 15(a) shows the relaxation properties of PET-TPE system, and the relaxation is centred around -60 °C on $\tan \delta$ peak and may be associated with the movement of

the aliphatic $(CH_2)_n$ segments. At high temperatures, the onset of the relaxation starts over the temperature of 0 °C and spans till 55 °C. This relaxation is associated with the coordinated movements of soft-hard domain of polymer chains. As seen from Figure 15(b), triazole system has obvious damping peak at approximate -19 °C, corresponding to the glass transition of the copolyether strands. When the tridimensional network is part of the semi-IENs, the most visible changes in the damping behavior are the decrease of the $\tan \delta$ peak at high temperatures. All these modifications come from entanglement between the chain and chain, and the linear PU domains are tightly embedded into the tridimensional network. The decrease of $\tan \delta$ value presents that the elastomers have excellent cryogenic property.

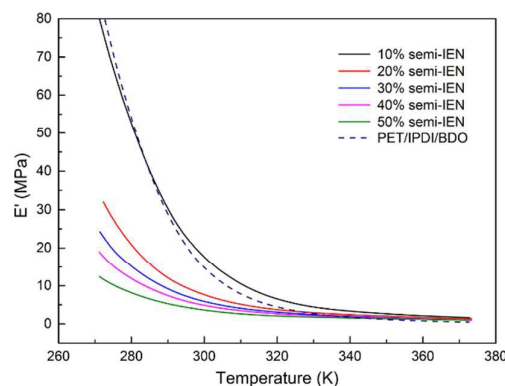


Fig. 11 Elastic modulus of semi-IENs (triazole system content is 10, 20, 30, 40, and 50 wt. %) as a function of temperature.

Table 2 Values of network structure parameters for semi-IENs (triazole system content is 10, 20, 30, 40, and 50 wt. %)

Sample	E_a^a (KJ/mol)	A^b	R^c	V_p^d (25°C)	E_p/E^e (25°C)
PET/IPDI/BDO	47.78	2.61×10^{-11}	0.9988	64.95	95%
Acyl-GAP/BPS	3.73	3.482	0.9956	1.568	40%
10% semi-IEN	46.22	5.96×10^{-7}	0.9999	74.54	95%
20% semi-IEN	38.19	6.01×10^{-6}	0.9995	29.43	90%
30% semi-IEN	32.97	3.85×10^{-5}	0.9992	23.0	88%
40% semi-IEN	32.01	4.57×10^{-5}	0.9993	18.54	87%
50% semi-IEN	34.27	1.23×10^{-5}	0.9989	12.46	81%

^a Calculated from Eq. (1), Eq. (4), Figure 10 and Figure 12 (b).

^b A is a pre-exponential factor, its physical significance is the value of physical crosslinking density when the temperature is infinite.

^c R is the correlation coefficient of fitting

^d Calculated from Eq. (1) when temperature is 25°C.

^e E_p/E is the percentage of the contribution of physical crosslinking in elastic modulus.

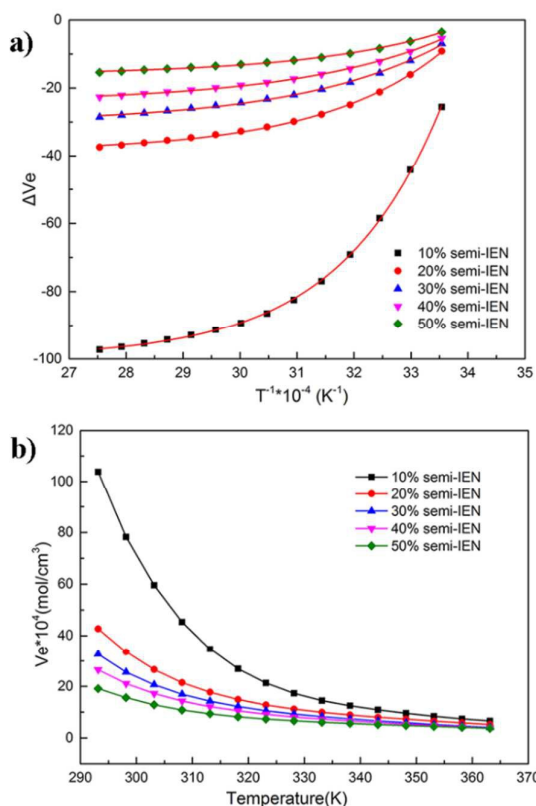


Fig. 12 Relationship between V_e and T , ΔV_e and $1/T$ of semi-IENs (triazole system content is 10, 20, 30, 40, and 50 wt. %). Lines are the regression results.

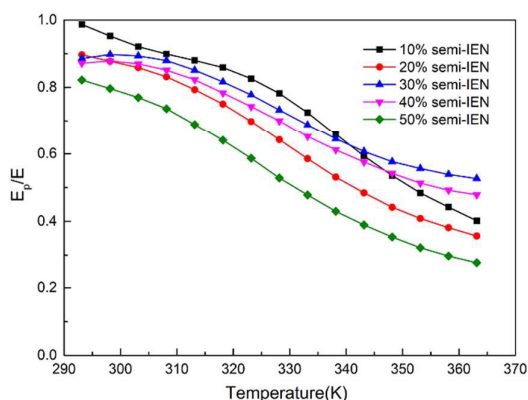


Fig. 14 Contribution of physical crosslinking of semi-IENs (triazole system content is 10, 20, 30, 40, and 50 wt. %) as a function of temperature.

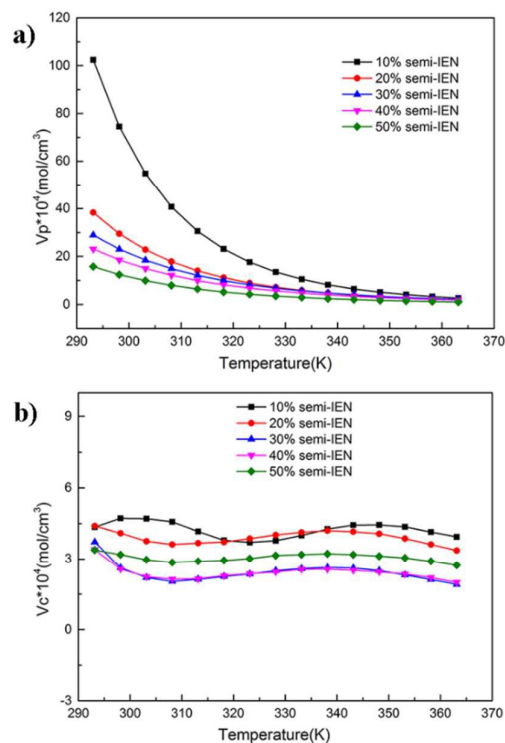


Fig. 13 Relationship between V_p , V_c and temperature of semi-IENs (triazole system content is 10, 20, 30, 40, and 50 wt. %).

Thermal stability of semi-IENs

The TG analysis was conducted to investigate the thermal stability of the prepared semi-IENs. Fig. 16 shows the TG and derivative thermo-gravimetric (DTG) curves of triazole system, PET-TPE and semi-IENs. As shown from Fig. 16(b), all samples of semi-IENs exhibit three steps thermal degradation, of which the temperatures range from 205 °C to 500 °C. The initial 5% weight loss for total semi-IENs occurs around 240 °C, suggesting that the samples have good thermal stability properties. Among them, the first step is about 205~282 °C, which is attributed to the thermal degradation of azide group and triazole ring; the second step is about 282~362 °C, which is attributed to the thermal degradation of polyether chain; the third step is about 362~500 °C, which is attributed to the thermal degradation of carbamate and other residual segment.

The corresponding decomposition temperatures obtained from TG-DTG curves are listed in Table 3. The results show that the maximum decomposition temperature of semi-IENs has increased to a certain extent compared with unitary system. The improvement of thermal stability is caused by the introduction of crosslinking network which supplies the shield effect during the thermal degradation. Normally, the $T_{\text{heat-resistance index}}$ (T_{HRI}) is recognized as an effective method to define the heat resistance of materials to ageing under the high temperature^{30, 31}. The higher T_{HRI} , the better thermal stability of the materials. The T_{HRI} can be expressed as Eq. (5):

$$T_{HRI} = 0.49 * [T_{d1} + 0.6(T_{d2} - T_{d1})] \quad \text{Eq. (4)}$$

The calculated T_{HRI} is also listed in Table 3. It's seen that after adding of triazole system into polyurethane matrix, the T_{HRI} of semi-IENs sample is located between pure PET-TPE and triazole system. This reveals that well interpenetrating structure have advantages for the heat resistance of the

triazole system. Although, the release of heat accelerate the decomposition of PET-TPEs, the semi-IENs still showed relatively high thermal stability.

Based on these results, the prepared semi-IENs are very stable in the temperature range for aerospace industry and missile technology.³²

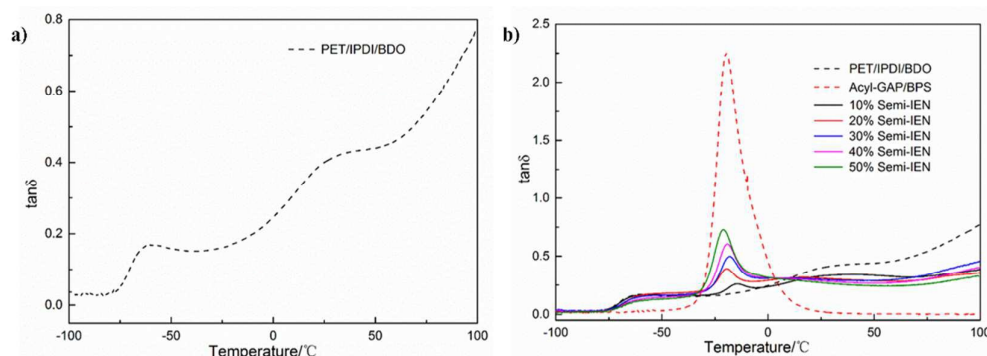


Fig. 15 Dependences of $\tan \delta$ on temperature. (a) PET/IPDI/BDO system; (b) Acyl-GAP/BPS and semi-IENs system. (triazole system content is 10, 20, 30, 40, and 50 wt. %).

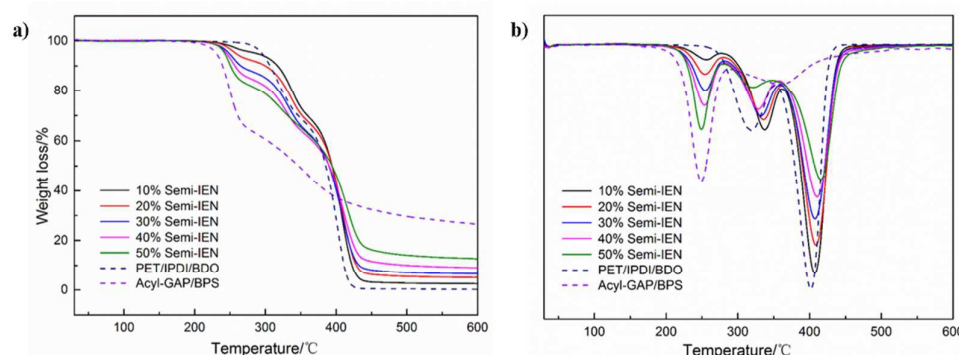


Fig. 16 TG and DTG curves of PET/IPDI/BDO, Acyl-GAP/BPS and semi-IENs. (triazole system content is 10, 20, 30, 40, and 50 wt. %).

Table 3 Thermal decomposition data of PET/IPDI/BDO, Acyl-GAP/BPS and semi-IENs. (triazole system content is 10, 20, 30, 40, and 50 wt. %)

Samples	First stage		Second stage		Third stage		Weight loss temperature/ $^{\circ}\text{C}$		$T_{HRI}/^{\circ}\text{C}$
	$T_{\max,1}^a$	$T_{\max,2}^b$	$T_{\max,3}^c$	T_{d1}^d	T_{d2}^e	T_{d1}^d	T_{d2}^e		
PET/IPDI/BDO	-	318.20	401.71	295.3	373.7			167.7	
Acyl-GAP/BPS	248.9	361.79	-	230.8	303.0			134.3	
10% semi-IEN	256.28	337.38	407.2	287.7	383.6			169.2	
20% semi-IEN	254.1	335.81	408.87	258.5	381.3			162.8	
30% semi-IEN	254.48	331.86	407.41	249.0	371.0			157.9	
40% semi-IEN	253.91	328.52	410.48	245.4	366.3			155.8	
50% semi-IEN	249.2	321.25	415.34	242.8	369.8			156.3	

^a The maximum decomposition temperature of the first decomposition stage.

^b The maximum decomposition temperature of the second decomposition stage.

^c The maximum decomposition temperature of the third decomposition stage.

^d The sample's decomposition temperature of 5% weight loss.

^e The sample's decomposition temperature of 40% weight loss.

Energy analysis

There is a positive correlation relationship between heat of decomposition and heat of combustion for binder. To further confirm the effect of triazole system on heat of formation, the heat of decomposition of samples are experimented and shown in Fig. 17 and Table 4. Obviously, the decomposition heat of semi-IENs increase from 256 to 1707 J/g with the content of triazole system increase. The results indicate that the semi-IENs have a high positive heat of formation, whose characteristics meet the requirements of the energetic binders.

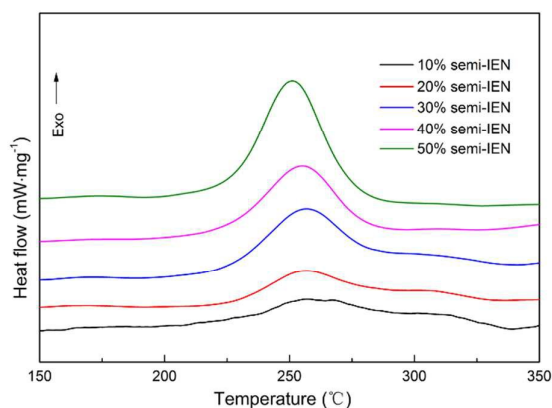


Fig. 17 DSC curves of semi-IENs. (triazole system content is 10, 20, 30, 40, and 50 wt. %)

Table 4 The decomposition heat of semi-IENs. (triazole system content is 10, 20, 30, 40, and 50 wt. %)

Samples	10% semi- IEN	20% semi- IEN	30% semi- IEN	40% semi- IEN	50% semi- IEN
Q^a (J/g)	256.43	301.74	813.44	1099.59	1707.6
T_p^b (°C)	257.22	256.21	255.36	254.76	251.14

^a The heat release of the samples.

^b The decomposition peak temperature of the samples.

Conclusions

A novel approach has been adopted in order to fabricate the excellent mechanical performance and energetic elastomer. A series of semi-IENs containing 10, 20, 30, 40 and 50 wt. % of triazole networks were synthesized via a sequential-IPN process in which the Acyl-GAP polymer along with cross-linker are swollen in already synthesized PET-TPE network and the two networks are noninterfering. When the mass percentage of triazole network is 20 wt. %, the prepared semi-IENs keep the maximal mechanical strength and elongation.

Network structure parameters are quantitative calculated based on the relationship between elastic modulus and

effective crosslinking density. The damping analysis results present that the linear PU domains are tightly embedded into the tridimensional network. It also can be confirmed from thermal stability and energy analysis that the sample exhibit good thermal stability and higher positive heat of formation. Based on all results, it is concluded that prepared semi-IENs can be considered as promising adhesives for aerospace industry and missile technology.

Conflicts of interest

There are no conflicts to declare.

Acknowledgements

Financial support for this work through the National Natural Science Foundation of China (NSFC) (Contract No. U1630142) is greatly appreciated.

References

- M. E. Colclough, H. Desai, R. W. Millar, N. C. Paul, M. J. Stewart and P. Golding, *Polym. Advan. Technol.*, 1994, **5**, 554-560.
- D. Bhowmik, V. S. Sadavarte, S. M. Pande and B. S. Saraswat, *Cent. Eur. J. Energ. Mater.*, 2015, **12**, 145-158.
- A. Davenas, *J. Propul. Power*, 2003, **19**, 1108-1128.
- A. Kanti Sikder and S. Reddy, *Propellants, Explos., Pyrotech.*, 2013, **38**, 14-28.
- S. Li, Y. Liu, X. Tuo and X. Wang, *Polymer*, 2008, **49**, 2775-2780.
- H. T., *Journal of Beijing Institute of Technology*, 1992, **51**.
- Y. Yang, Y. J. LUO, J. R. Liu and Z. GE, *Fine Chem.*, 2008, **2**, 005.
- A. Nazare, S. Asthana and H. Singh, *J. Energ. Mater.*, 1992, **10**, 43-63.
- S. Manu, T. Varghese, S. Mathew and K. Ninan, *J. Appl. Polym. Sci.*, 2009, **114**, 3360-3368.
- T. H. Hagen, T. L. Jensen, E. Unneberg, Y. H. Stenstrom and T. E. Kristensen, *Propellants, Explos. Pyrotech.*, 2015, **40**, 275-284.
- A. Abirami, R. Soman, N. Agawane, J. G. Bhujbal, R. Singh and P. S. Kulkarni, *Inter. J. Energ. Mater. Chem. Propul.*, 2016, **15**.
- S. H. Sonawane, S. Banerjee, A. K. Sider, M. B. Talawar and M. A. S. Khan, *New J. Chem.*, 2017, **41**, 7886-7892.
- D.-H. Lee, K. T. Kim, H. Jung, S. H. Kim, S. Park, H. B. Jeon, H.-j. Paik, B. S. Min and W. Kim, *J. Taiwan Inst. Chem. Eng.*, 2014, **45**, 3110-3116.
- B. S. Min, C. K. Kim, M. S. Ryoo and S. Y. Kim, *Fuel*, 2014, **136**, 165-171.
- S. Reshmi, H. Hemanth, S. Gayathri and C. R. Nair, *Polymer*, 2016, **92**, 201-209.
- H. Li, Q. Yu, F. Zhao, B. Wang and N. Li, *J. Appl. Polymer. Sc.*, 2017.
- C. R. Rao, R. Narayan and K. Raju, *Micro-and Nano-Structured Interpenetrating Polymer Networks: From Design to Applications*, 2016, **80**, 259.
- A. Ravve, *Principles of polymer chemistry*, Springer Science & Business Media, 2013.
- L. H. Sperling, *Interpenetrating polymer networks and related materials*, Springer Science & Business Media, 2012.

NJC

Paper

20. J. W. Nicholson, *J. Mater. Chem.*, 2006, **16**, 3867-3874.
21. A. Tanver, M.-H. Huang, Y. Luo, S. Khalid and T. Hussain, *RSC Adv.*, 2015, **5**, 64478-64485.
22. T. Keicher, W. Kuglstatler, S. Eisele, T. Wetzel and H. Krause, *Propellants Explos. Pyrotech.*, 2009, **34**, 210-217.
23. A. Pangon, G. P. Dillon and J. Runt, *Polymer*, 2014, **55**, 1837-1844.
24. M. Bruma, M. Cristea, S. Ibanescu, C. N. Cascaval and D. Rosu, *High Perform. Polym.*, 2009, **21**, 608-623.
25. S. Qiu, X. Gan, C. Gao, X. Zheng, H. Yu and H. Fan, *J. Polym. Sci. Polym. Phys.*, 2006, **44**, 2841-2851.
26. L. Weisfeld, J. Little and W. Wolstenholme, *J. Polym. Sci.*, 1962, **56**, 455-463.
27. S. Xu, B. Chen, T. Tang and B. Huang, *Polymer*, 1999, **40**, 3399-3406.
28. L. Zhang and S. J. Rowan, *Macromolecules*, 2017, **50**, 5051-5060.
29. M. Furukawa, Y. Mitsui, T. Fukumaru and K. Kojio, *Polymer*, 2005, **46**, 10817-10822.
30. C. Liang, P. Song, H. Gu, C. Ma, Y. Guo, H. Zhang, X. Xu, Q. Zhang and J. Gu, *Composites Part A: Applied Science and Manufacturing*, 2017, **102**, 126-136.
31. J. Gu, W. Dong, Y. Tang, Y. Guo, L. Tang, J. Kong, S. Tadakamalla, B. Wang and Z. Guo, *J. Mater. Chem. C*, 2017.
32. L. Mallick, S. Lal, S. Reshmi, I. N. Namboothiri, A. Chowdhury and N. Kumbhakarna, *New Journal of Chemistry*, 2017.

NJC

PAPER

Preparation and properties of semi-interpenetrating networks combined by thermoplastic polyurethane and thermosetting elastomer

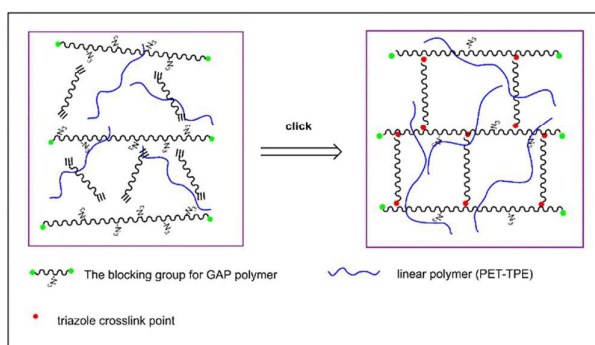
Received 00th January 20xx,
Accepted 00th January 20xx

DOI: 10.1039/x0xx00000x

www.rsc.org/

Yajin Li,^a Guoping Li^a, Jie Li and Yunjun Luo^{*a}

Table of Content Entry



A novel energetic macromolecule of semi-interpenetrating materials were prepared via sequential-IPN process, which can be used in the area of aerospace industry and missile technology.

^a School of Materials Science & Engineering, Beijing Institute of Technology, Beijing 100081, PR China. E-mail: yjluo@bit.edu.cn; Fax: +86 010 68913698; Tel: +86 010 68913698.

Electronic Supplementary Information (ESI) available: [details of any supplementary information available should be included here]. See DOI: 10.1039/x0xx00000x